Synthesis and Structural Characterization of a Bitopic Ferrocenyl-Linked Bis(pyrazolyl)methane Ligand and Its Silver(I) Coordination Polymers

Daniel L. Reger,* Kenneth J. Brown, James R. Gardinier, and Mark D. Smith

Department of Chemistry and Biochemistry, University of South Carolina, Columbia, South Carolina 29208

Received July 3, 2003

The bitopic ligand 1,1′-bis(dipyrazol-1-ylmethyl)ferrocene, $Fe[C_5H_4CH(pz)_2]_2$ (**1**; pz = pyrazolyl ring), has been prepared by the reaction of 1,1′-ferrocenedicarbaldehyde and 1,1′-carbonyldipyrazole. In the solid state, the bis(pyrazolyl)methane moieties are in an antiperiplanar eclipsed orientation. The molecules are organized into a three-dimensional array by $\pi\cdots\pi$, weak C−H···N hydrogen bonding, and C−H···π interactions. The reactions between **1** and $AgBF_4$, $AgPF_6$, $AgSO_3CF_3$, or $AgSbF_6$ yield $\{Fe[C_5H_4CH(pz)_2]_2AgBF_4\}_n$ (**2**), $\{Fe[C_5H_4CH(pz)_2]_2AgPF_6\}_n$ (**3**), $\{Fe[C_5H_4CH(pz)_2]_2AgSO_3CF_3\}_n$ (**4**), and $\{Fe[C_5H_4CH(pz)_2]_2AgSbF_6\}_n$ (**5**), respectively. The solid-state structures consist of coordination polymers with compounds **2** and **3** arranged in helical chains, while the chains in **3**·$^1/_2Et_2O$, **4**·$1.5C_6H_6$, **5**·$^1/_2Et_2O$, and **5**·$^1/_2C_6H_6$ are nonhelical. In these structures, the ferrocenyl groups adopt a similar orientation, where the angle between $CH(pz)_2$ groups is confined to the range of 85−99° and the silver pyrazolyl coordination spheres are also in very similar distorted-tetrahedral arrangements. Both structural types form three-dimensional supramolecular structures organized by weak hydrogen bonds, $\pi\cdots\pi$ stacking, and CH···π interactions. In the helical form, the anions reside in the pockets formed by the close-packed chains, whereas in the nonhelical form, sizable channels, which contain the solvent molecules and the anions, are located between the chains.

Introduction

Over the past decade immense interest has been generated in the development of coordination network solids for their potential both in materials chemistry and in catalysis.[1] Key to the development of this field has been the ability to design multitopic ligands that are capable of binding to metal centers in a predictable manner defined by the geometry of the ligand. Our research group has been interested in the development and use of semirigid, multitopic organic-linked poly(pyrazolyl)methane compounds as potential connectors for coordination networks. Recently we reported the synthesis of the first linked bis(pyrazolyl)methane ligand $CH_2[CH(pz)_2]_2$ (pz = pyrazolyl ring) and explored its coordination chemistry with silver(I).[2] This ligand was found to bridge silver centers to form discrete bi- and trimetallic species, rather than forming coordination networks. These discrete multimetallic silver species were found to be organized into supramolecular structures in the solid state as a result of a set of cooperative $\pi\cdots\pi$ and CH···π interactions that were termed the "quadruple pyrazolyl embrace". As a continuation of the above studies, our research group has been exploring the effects of introducing specific spacers other than the methylene unit in linked bis(pyrazolyl)methane ligands on both the coordination capabilities and supramolecular assembly of metal complexes. The ferrocenyl moiety has proven to be an excellent choice for incorporation into polymers and coordination network solids because of its interesting electrochemical properties and its ability to provide structural diversity as a result of conformational flexibility.[3] Specifically, coordination complexes of bitopic 1,1′-ferrocenyl ligands have several possible structural types, including discrete molecular units,[4] discrete cyclic species,[5] linear chains,[6] and helix-like chains.[7] Wagner's group has previously reported the development of several mono- and bitopic

* To whom correspondence should be addressed. E-mail: reger@mail.chem.sc.edu.

(1) (a) Evans, O. R.; Lin, W. *Acc. Chem. Res.* **2002**, *35*, 511. (b) Braga, D. *J. Chem. Soc., Dalton Trans.* **2000**, *21*, 3705. (c) Lee, S. J.; Hu, A.; Lin, W. *J. Am. Chem. Soc.* **2002**, *124*, 12948.

(2) Reger, D. L., Gardinier, J. R., Semeniuc, R. F., Smith, M. D. *J. Chem. Soc., Dalton Trans.* **2003**, 1712.

(3) (a) Dong, T.-Y.; Huang, B.-R.; Lin, M.-C.; Chiang, M. Y. *Polyhedron* **2003**, *22*, 1199. (b) Constable, E. C. *Prog. Inorg. Chem.* **1994**, *42*, 67. (c) Constable, E. C.; Edwards, A. J.; Raithby, P. R.; Walker, J. V. *Angew. Chem.* **1993**, *32*, 1465 and references therein. (d) Constable, E. C.; Daniels, M. A. M.; Drew, M. G. B.; Tocher, D. A.; Walker, J. V.; Wood, P. D. *J. Chem. Soc., Dalton Trans.* **1993**, 1947 and references therein. (e) Constable, E. C. *Tetrahedron* **1992**, *48*, 10013 and references therein. (f) Potts, K. T.; Keshavarz-K, M.; Tham, F. S.; Abruna, H. D.; Arana, C. *Inorg. Chem.*, **1993**, *32*, 4422, 4436, 4450. (g) Potts, K. T.; Keshavarz-K, M.; Raiford, K. A. G.; Tham, F. S.; Arana, C.; Abruna, H. D. *Inorg. Chem.* **1993**, *32*, 5477. (h) Hudson, R. D. A. *J. Organomet. Chem.* **2001**, *637−639*, 47. (i) Dong, G.; Yu-ting, L.; Chunying, D.; Hong, M.; Qing-jin, M. *Inorg. Chem.* **2003**, *42*, 2519.

(4) (a) Barranco, E. M.; Crespo, O.; Gimeno, M. C.; Jones, P. G.; Laguna, A.; Sarroca, C. *J. Chem. Soc., Dalton Trans.*, **2001**, 2523. (b) Hui, J. W.-S.; Wong, W.-T. *J. Chem. Soc., Dalton Trans.* **1997**, 2445. (c) Mai, J.-F.; Yamamoto, Y. *J. Organomet. Chem.* **1998**, *560*, 223.

(5) (a) Braga, D.; Polito, M.; Bracaccini, M.; D'Addario, D.; Tagliavini, E.; Proserpio, D. M.; Grepioni, F. *Chem. Commun.* **2002**, 1080. (b) Cotton, F. A.; Daniels, L. M.; Lin, C.; Murillo, C. A. *J. Am. Chem. Soc.* **1999**, *121*, 4538.

10.1021/om0305216 CCC: $25.00
Publication on Web 10/23/2003

Scheme 1

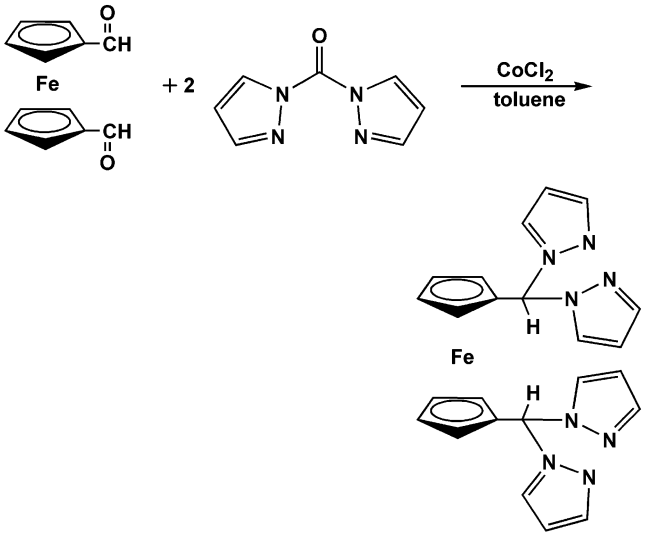

ferrocene-based poly(pyrazolyl)borate ligands.[8] To the best of our knowledge, there is only one example of the incorporation of a ferrocene unit into the backbone of a poly(pyrazolyl)methane ligand.[9] We now report on the preparation of the first of a series of ferrocenyl-linked poly(pyrazolyl)methane ligands, 1,1′-bis(dipyrazol-1-ylmethyl)ferrocene, $Fe[C_5H_4CH(pz)_2]_2$, and detail the structural diversity found in its silver(I) complexes.

Results and Discussion

The reaction of 1,1′-ferrocenyldicarbaldehyde[10] and 1,1′-carbonyldipyrazole[11] in toluene in the presence of a catalytic amount of anhydrous cobalt(II) chloride results in the formation of 1,1′-bis(dipyrazol-1-ylmethyl)-ferrocene ($Fe[C_5H_4CH(pz)_2]_2$, **1**) (Scheme 1). This procedure has been used previously to prepare the monotopic ligand [bis(3,5-dimethylpyrazol-1-yl)methyl]ferrocene.[9] The orange crystalline solid **1** is air stable and is readily soluble in acetone, THF, methylene chloride, toluene, and acetonitrile, while being only very slightly soluble in diethyl ether and hexane.

As a basis for comparison of the orientations of the bis(pyrazolyl)methane units, two torsion angles will be discussed. The first torsion angle, τ_1, is a measure of the rotation of the H(1)−C(1) (or H(2)−C(2)) bond out of the plane of the cyclopentadienyl (Cp) ring to which it is attached (Figure 1). The second torsion angle, τ_2, determines the rotation of the bis(pyrazolyl)methane units on the Cp rings of the ferrocene unit about the Cp(centroid)−Fe−Cp(centroid) axis[12] (Figure 2). The angles τ_1 and τ_2 were determined using "ORTEP-3 for Windows version 1.076",[13] and the signs are based on the conventions within the program.

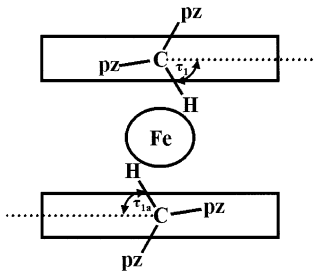

Figure 1. Torsion angle τ_1, a measure of the rotation of the C−H bond out of the plane of the Cp ring to which it is attached.

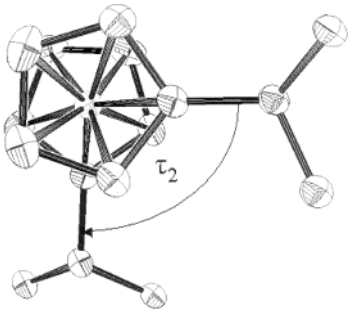

Figure 2. Torsion angle τ_2, a measure of the rotation of the bis(pyrazolyl)methane units about the Cp(centroid)−Fe−Cp(centroid) axis.

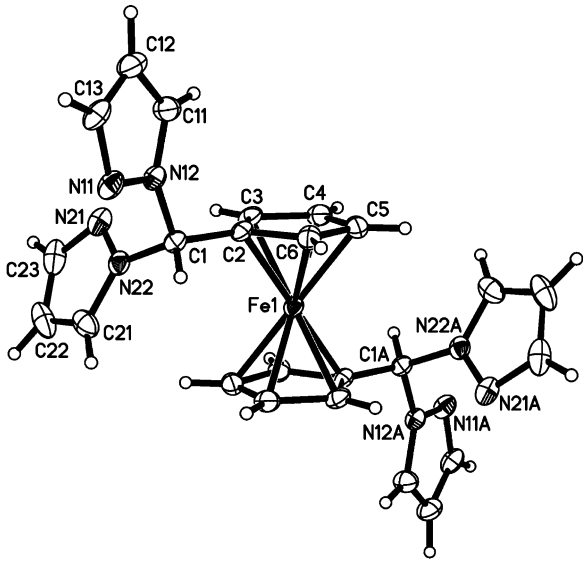

Figure 3. ORTEP diagram showing the atom-numbering scheme for **1**. Thermal ellipsoids are at the 50% probability level.

Solid-State Structure of 1. Figure 3 shows an ORTEP diagram of one of the two crystallographically nonequivalent forms of **1**, both of which are centrosymmetric, and selected bond distances and angles are

(6) (a) Gimeno, M. C.; Jones, P. G.; Laguna, A.; Sarroca, C. *J. Chem. Soc., Dalton Trans.* **1998**, 1*277*. (b) Houlton, A.; Mingos, D. M. P.; Murphy, D. M.; Williams, D. J.; Phang, L. T.; Hor, T. S. A. *J. Chem. Soc., Dalton Trans.* **1993**, 3629. (c) Horikoshi, R.; Ueda, M.; Mochida, T. *New J. Chem.* **2003**, *27*, 933. (d) Yuan, Y.-F.; Ye, S.-M.; Zhang, L.-Y.; Wang, J.-T. *Transition Met. Chem.* **1997**, *22*, 561.

(7) Horikoshi, R.; Mochida, T.; Moriyama, H. *Inorg. Chem.* **2002**, *41*, 3017.

(8) (a) Jakle, F.; Polborn, K.; Wagner, M. *Chem. Ber.* **1996**, *129*, 603. (b) Fabrizi de Biani, F.; Jakle, F.; Spiegler, M.; Wagner, M.; Zanello, P. *Inorg. Chem.* **1997**, *36*, 2103. (c) Herdtweck, E.; Peters, F.; Scherer, W.; Wagner, M. *Polyhedron* **1998**, *17*, 1149. (d) Guo, S. L.; Peters, F.; Fabrizi de Biani, F.; Bats, J. W.; Herdtweck, E.; Zanello, P.; Wagner, M. *Inorg. Chem.* **2001**, *40*, 4928.

(9) Carrion, M. C.; Diaz, A.; Guerrero, A.; Jalon, F. A.; Manzano, B. R.; Rodriguez, A. *New J. Chem.* **2002**, *26*, 305.

(10) Balavoine, G. G. A.; Doisneau, G.; Fillebeen-Khan, T. *J. Organomet. Chem.* **1991**, *412*, 381.

(11) Byers, P. K.; Canty, A. J.; Honeyman, R. T. *J. Organomet. Chem.* **1990**, *385*, 417.

(12) Gan, K. S.; Hor, T. S. A. 1, 1′-Bis(diphenylphosphino)ferrocene−Coordination Chemistry, Organic Syntheses, and Catalysis. In *Ferrocenes: Homogeneous Catalysis, Organic Synthesis, Material Science*; Togni, A., Hayashi, T., Eds.; VCH: Weinheim, Germany, 1995; pp 3−104.

(13) Farrugia, L. J. *J. Appl. Crystallogr.* **1997**, *30*, 565.

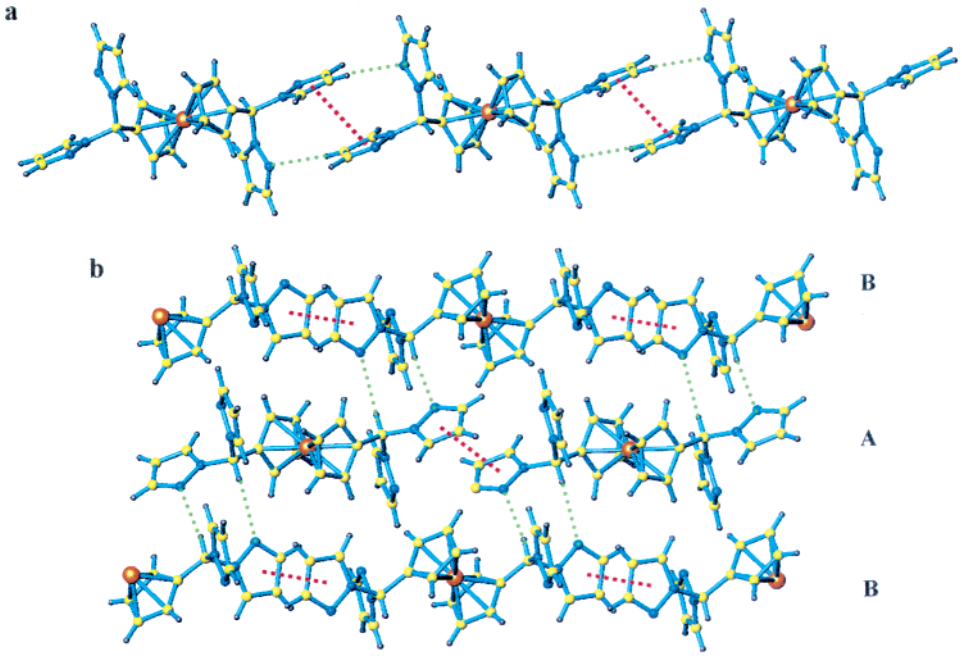

Figure 4. (a) Three molecular units of chain **A** of $Fe[C_5H_4CH(pz)_2]_2$ (**1**) showing $\pi\cdots\pi$ (red hashes) and CH···N (green dots) interactions. (b) Three chains of **1** showing CH···N interchain interactions (green dots) that hold the **A** and **B** chains together in sheets. The $\pi\cdots\pi$ (red hashes) interactions are the same interactions shown in Figure 4a.

Table 1. Selected Bond Lengths (Å) and Angles (deg) for Each of the Two Independent Molecules of 1 within the Crystal

	A	B
C(1)−N(12)	1.457(2)	1.459(2)
C(1)−N(22)	1.456(2)	1.456(2)
N(12)−C(1)−C(2)	111.77(13)	112.40(13)
N(22)−C(1)−C(2)	112.76(13)	113.35(13)
N(12)−C(1)−N(22)	110.35(13)	110.01(13)

collected in Table 1. The pyrazolyl rings of each bis(pyrazolyl)methane unit are oriented away from each other and from the cyclopentadienyl ring with τ_1 angles of −35 and −27° for each of the two molecules in the crystal. Both molecules in the crystal of **1** also have their bis(pyrazolyl)methane moieties in an antiperiplanar eclipsed orientation, corresponding to a τ_2 angle of 180°.[12]

The two crystallographically independent molecules, **A** and **B**, form two nearly identical chains that propagate along the crystallographic *c* axis. Figure 4a shows chain **A** (chain **B** is similar). Each chain is held together by a parallel displaced $\pi\cdots\pi$ interaction[14] between a pyrazolyl ring from one molecule and the symmetry-equivalent pyrazolyl ring from a neighboring molecule. For chain **A**, the centroid···centroid (Cg···Cg) distance of the $\pi\cdots\pi$ interaction is 3.64 Å, and for chain **B** the Cg···Cg distance is 3.68 Å. This interaction is supported by a weak C−H···N interaction.[15] For each chain, the hydrogen atom at the 3-position on the pyrazolyl ring involved in $\pi\cdots\pi$ stacking is directed toward the nitrogen atom lone pair on the pyrazolyl ring of an adjacent molecule that is not involved in the $\pi\cdots\pi$ stacking. For **A**, the H(13)···N(21) distance is 2.61 Å with a C(13)···N(21) distance of 3.33 Å and a C(13)−H(13)···N(21) angle of 133°, while for **B**, the H(43)···N(51) distance is 2.73 Å with a C(43)···N(51) distance of 3.39 Å and a C(43)−H(43)···N(51) angle of 127°.

Figure 4b shows the further organization of the chains into two-dimensional sheets that are held together by a second set of weak C−H···N hydrogen-bonding interactions. The lone pair of a nitrogen atom of the pyrazolyl rings that are involved in the $\pi\cdots\pi$ stacking are directed toward the methine hydrogen atom of a molecular unit from the adjacent chain. For the **A** methine hydrogen atom to **B** nitrogen atom interaction, the H(1)···N(41) distance is 2.66 Å with a C(1)···N(41) distance of 3.49 Å and a C(1)−H(1)···N(41) angle of 150°. For the **B** methine hydrogen atom to **A** nitrogen atom interaction, the H(31)···N(11) distance is 2.42 Å with a C(31)···N(11) distance of 3.33 Å and a C(31)−H(31)···N(11) angle of 170°.

The sheets are further organized into a three-dimensional array by C−H···π interactions (Figure 5).[16] The hydrogen atom in chain **B** at the 4-position of the pyrazolyl ring, which does not partake in $\pi\cdots\pi$ stacking, is aimed at the π-cloud of the pyrazolyl ring, which is involved in $\pi\cdots\pi$ stacking in chain **A**. The H(52)···Cg distance is 2.78 Å with a C(52)···Cg distance of 3.55 Å and a C(52)−H(52)···Cg angle of 139°.

Syntheses of $\{Fe[C_5H_4CH(pz)_2]_2AgX\}_n$ Complexes. The reaction between **1** and $AgBF_4$, $AgPF_6$, $AgSO_3CF_3$, or $AgSbF_6$ in a 1:1 mole ratio in THF results in the precipitation of $\{Fe[C_5H_4CH(pz)_2]_2AgBF_4\}_n$ (**2**), $\{Fe[C_5H_4CH(pz)_2]_2AgPF_6\}_n$ (**3**), $\{Fe[C_5H_4CH(pz)_2]_2AgSO_3CF_3\}_n$ (**4**), and $\{Fe[C_5H_4CH(pz)_2]_2AgSbF_6\}_n$ (**5**), respec-

(14) Janiak, C. *J. Chem. Soc., Dalton Trans.* **2000**, 3885 and references therein.

(15) (a) Bondi, A. *J. Phys. Chem.* **1964**, *68*, 441. (b) Rowland, R. S.; Taylor, R. *J. Phys. Chem.* **1996**, *100*, 7384.

(16) (a) Takahashi, H.; Tsuboyama, S.; Umezawa, Y.; Honda, K.; Nishio, M. *Tetrahedron* **2000**, *56*, 6185. (b) Tsuzuki, S.; Honda, K.; Uchimaru, T.; Mikami, M.; Tanabe, K. *J. Am. Chem. Soc.* **2000**, *122*, 11450. (c) Seneque, O.; Giorgi, M.; Reinaud, O. *Chem. Commun.* **2001**, 984. (d) Weiss, H. C.; Blaser, D.; Boese, R.; Doughan, B. M.; Haley, M. M. *Chem. Commun.* **1997**, 1703 (e) Madhavi, N. N. L.; Katz, A. K.; Carrell, H. L.; Nangia, A.; Desiraju, G. R. *Chem. Commun.* **1997**, 2249 (f) Madhavi, N. N. L.; Katz, A. K.; Carrell, H. L.; Nangia, A.; Desiraju, G. R. *Chem. Commun.* **1997**, 1953.

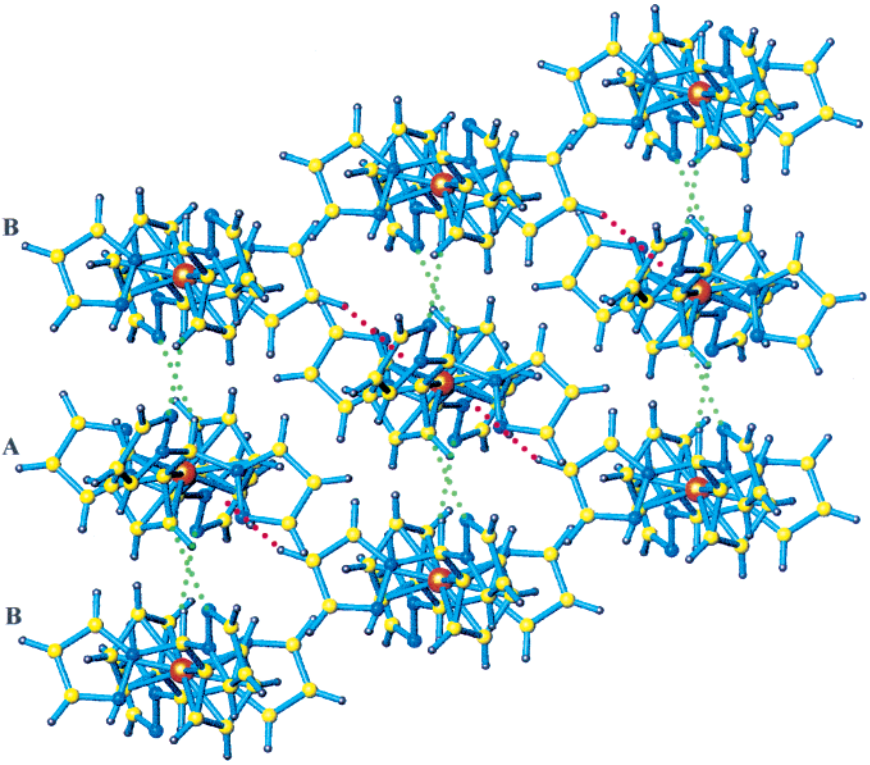

Figure 5. View orthogonal to Figure 4b showing the two-dimensional sheets in **1** formed through CH···N interactions (green dots). Shown here is an array of three sheets held together into a three-dimensional network by CH···π interactions (red dots).

tively, as yellow solids (Scheme 2). The ESI^+ mass spectrum of each silver complex shows signals for a dimeric unit corresponding to $[Ag_2L_2X]^+$ (L = $Fe[C_5H_4CH(pz)_2]_2$) along with peaks for monometallic $[AgL_2]^+$ and $[AgL]^+$ species, while the spectrum for **4** also shows an additional peak corresponding to $[Ag_2LSO_3CF_3]^+$. These peaks indicate the formation of coordination polymers in solution,[17] as observed in the solid state (vide infra). As expected from the lability of silver pyrazolyl complexes, the ^1H and ^{13}C NMR spectra of each complex show only one set of resonances that are shifted downfield from those of the free ligand.

Solid-State Structures of $\{Fe[C_5H_4CH(pz)_2]_2AgX\}_n$ Complexes. The complexes **2**−**5** were crystallized by a variety of vapor phase diffusion and layering techniques (see the Experimental Section). In the case of **3**, vapor-phase diffusion of ether into an acetonitrile solution led to the formation of two crystalline forms. Figure 6 shows an ORTEP diagram of a fragment of the chain formed by **3**. The atom-numbering scheme shown is applicable to all the silver coordination polymers, and selected bond distances and angles are collected in Table 2. In all of the complexes, the ligand and silver cations form infinite one-dimensional chains; however, the chains in **2** and **3** are helical, while the chains in **3**·$^1/_2$-Et_2O, **4**·$1.5C_6H_6$, **5**·$^1/_2Et_2O$, and **5**·$^1/_2C_6H_6$ are nonhelical.

The major difference in the helical and nonhelical forms is the relative orientation of the ferrocenyl units in the polymer chains. Figure 7 shows fragments of **3** and **3**·$^1/_2Et_2O$ that depict the conformations of the chains (hydrogen and pyrazolyl carbon atoms have been omitted for clarity), while cartoons that illustrate the ferrocenyl stacking are shown to the right of each chain. An alternating AB orientation of the repeating ferrocenyl units is observed in **3** (Figure 7a), while a repeating AA orientation of the ferrocenyl units is found in **3**·$^1/_2$-Et_2O (Figure 7b). The other helical complex, **2**, also exhibits the AB ordering of the ferrocenyl units, while

Scheme 2

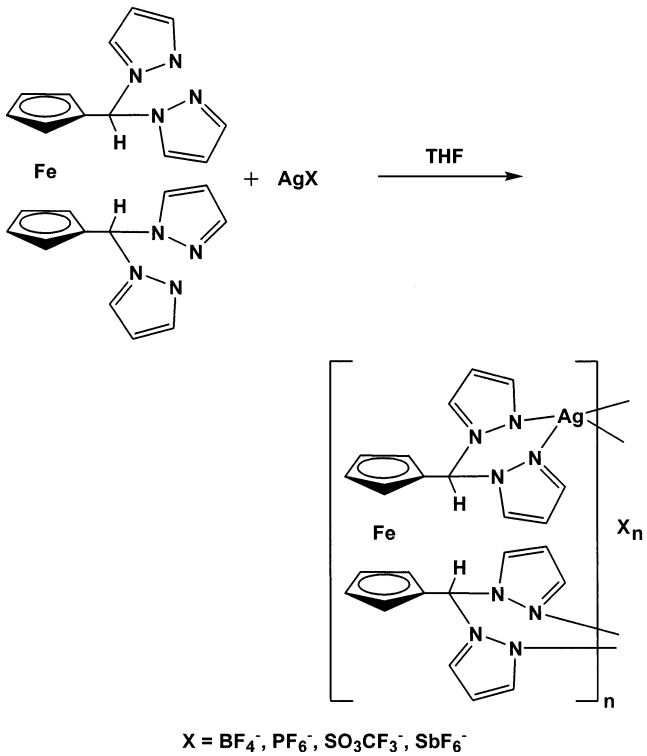

(17) Reger, D. L.; Semeniuc, R. F.; Silaghi-Dumitrescu, I.; Smith, M. D. *Inorg. Chem.* **2003**, *42*, 3751.

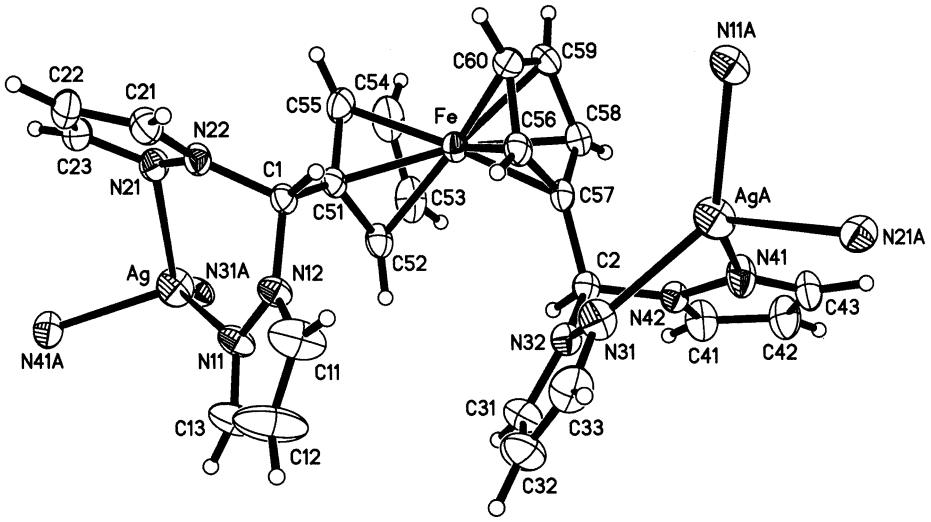

Figure 6. ORTEP diagram of a fragment of the chain repeat unit in $\{Fe[C_5H_4CH(pz)_2]_2AgPF_6\}_n$ (**3**). Displacement ellipsoids are drawn at the 50% probability level. The atom-numbering scheme shown is also correct for **2**, **3**·$^1/_2Et_2O$, **4**·1.5C_6H_6, **5**·$^1/_2Et_2O$, and **5**·$^1/_2C_6H_6$.

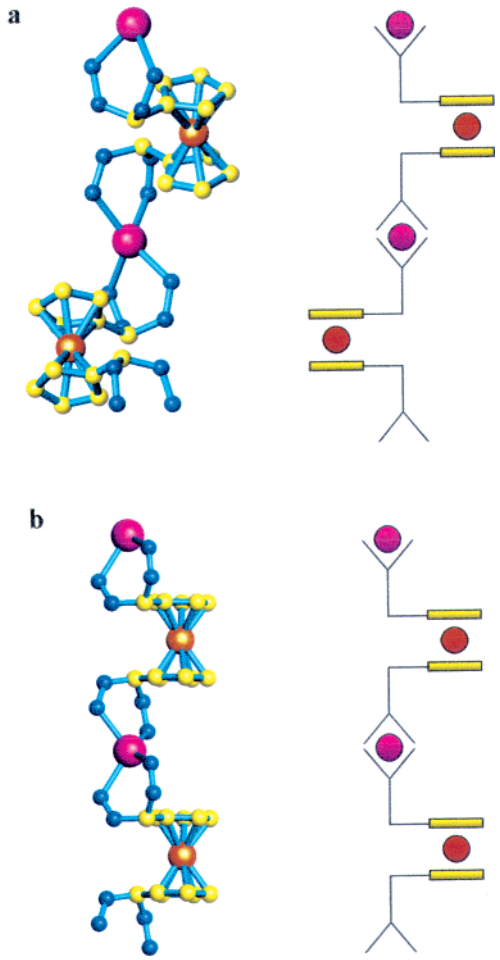

Figure 7. Chain fragments from **3** (a) and **3**·$^1/_2Et_2O$ (b) that show the different stacking arrangements of the two types of chains. Cartoon depictions of the stacking are given to the right of each chain. Hydrogen and pyrazolyl carbon atoms have been omitted for clarity.

the remaining nonhelical complexes, **4**·1.5C_6H_6, **5**·$^1/_2$-Et_2O, and **5**·$^1/_2C_6H_6$, are arranged in an AA orientation.

Despite the differences in the stacking of the two types of chains, the ligand orientation in each complex is surprisingly similar. Since the ligand subunit for each complex has two crystallographically inequivalent methine protons, there are two values for the torsion angle τ_1 for each silver complex which correspond to H(1)−C(1)−C(51)−C(55) and H(2)−C(2)−C(57)−C(58). The τ_1 angles for the helical type chains are −72 and −66° for **2** and −72 and −64° for **3**, resulting in an overall average τ_1 angle for the helical chains of −68°. The nonhelical complexes have τ_1 angles of −60 and −71° for **3**·$^1/_2Et_2O$, −69 and −75° for **4**·1.5C_6H_6, −62 and −69° for **5**·$^1/_2Et_2O$, and −60 and −68° for **5**·$^1/_2C_6H_6$, giving a nearly identical average τ_1 angle of −67°. In both cases, the H(1)−C(1) and H(2)−C(2) bonds are tilted to a greater degree than they are in the free ligand. The larger angle orients the pyrazolyl rings above the planes of the Cp rings, away from the iron center, to a greater degree than observed in the free ligand.

The rotations of the bis(pyrazolyl)methane units with respect to one another about the ferrocenyl unit are also surprisingly similar in the two types of structures but very different from that of the free ligand. The τ_2 angles for the helical complexes are 91° for **2** and 85° for **3**, yielding an average of 88°, while the separation between the bis(pyrazolyl)methane units for **3**·$^1/_2Et_2O$, **4**·1.5C_6H_6, **5**·$^1/_2Et_2O$, and **5**·$^1/_2C_6H_6$ are 96, 88, 93, and 99, respectively, giving an average of 94°. All of the silver complexes have τ_2 angles that fall between the ranges of the synclinal eclipsed (72°) and the anticlinal staggered (108°) arrangements.[12] The large τ_1 angles make any steric interactions between the bis(pyrazolyl)-methane units in each ligand negligible for any value of τ_2.

In addition to the fact that the ligand orientations are nearly identical in all of the complexes, the environments around the silver atoms are also similar. In all of the complexes, the silver cation is in a distorted-tetrahedral arrangement. The average Ag−N distance is 2.32 Å for **2**, **3**, and **3**·$^1/_2Et_2O$, 2.31 Å for **4**·1.5C_6H_6, and 2.33 Å for **5**·$^1/_2Et_2O$ and **5**·$^1/_2C_6H_6$. In each of the four complexes, one of the Ag−N distances for each bis-(pyrazolyl)methane unit is longer. The ranges for the Ag−N distances are 0.08 , 0.12 , 0.16 , 0.18 , 0.17 , and 0.11 Å for **2**, **3**, **3**·$^1/_2Et_2O$, **4**·1.5C_6H_6, **5**·$^1/_2Et_2O$, and **5**·

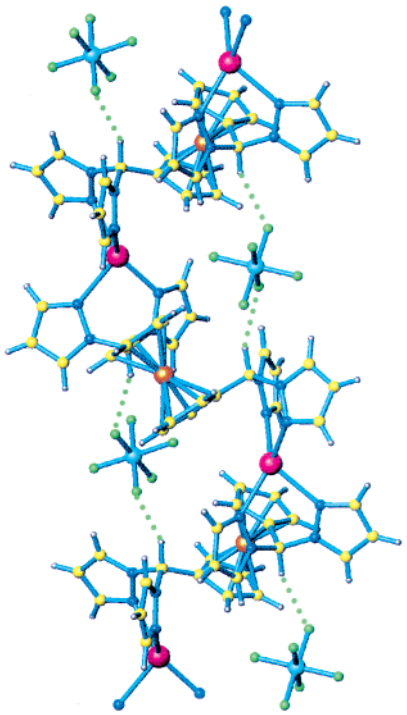

Figure 8. View of a single, helical chain from **3** with PF_6^- anions located in the pockets of the helix. The intrachain CH···F contacts are shown as green dots.

$^1/_2C_6H_6$, respectively. The longest Ag−N bond occurs in **5**·$^1/_2Et_2O$ with a Ag−N(11) distance of 2.420(4) Å, and the shortest Ag−N bond occurs in **4**·$1.5C_6H_6$, where the Ag−N(41) bond measures 2.225(3) Å.

Supramolecular Structures. Since the helical cationic chains in complexes **2** and **3** are isostructural and the structures of the nonhelical complexes **3**·$^1/_2Et_2O$, **4**·$1.5C_6H_6$, **5**·$^1/_2Et_2O$, and **5**·$^1/_2C_6H_6$ are similar to one another, the supramolecular structures of only **3** and **3**·$^1/_2Et_2O$ will be discussed in detail here. The remaining complexes will be detailed in the Supporting Information.

{Fe[$C_5H_4CH(pz)_2$]$_2$AgPF$_6$}$_n$ (3). The cationic coordination polymer in **3** forms one-dimensional, helical chains that propagate along the crystallographic *b* axis. Both right- and left-handed helices are present in the centrosymmetric (racemic) crystal. The chains are close-packed with the PF_6^- anions residing in the pockets created by the helices. There are several short CH···F contacts between the two methine hydrogens of each ligand and fluorine atoms of two anions (Figure 8) that are within the sum of their van der Waals radii (2.56 Å).[15]

The H(1)···F(1) distance is 2.33 Å, with a C(1)···F(1) distance of 3.27 Å and a C(1)−H(1)···F(1) angle of 156°; the other interaction has a H(2)···F(5) distance of 2.32 Å with a C(2)···F(5) distance of 3.27 Å and a C(2)−H(2)···F(5) angle of 158°. The distances and angles of these CH···F interactions are in good agreement with the typical geometric values (<2.6 Å and >130°) proposed to be indicative of weak hydrogen-bonding interactions involving the hexafluorophosphate anion.[18]

Figure 9a shows three chains of **3**, and Figure 9b shows a view down the three chains shown in Figure 9a. The right- and left-handed helical chains in **3** are held together in two-dimensional sheets by the "quadruple pyrazolyl embrace" (Figure 9c). The Cg···Cg distance for the $\pi\cdots\pi$ interaction of the pyrazolyl embrace is 4.21 Å with a β slip angle of 18°. The corresponding CH···π interaction has a H(12)···Cg distance of 3.10 Å with a C(12)···Cg distance of 3.70 Å and a C(12)−H(12)···Cg angle of 123°. These distances and angles are at the upper limits of the ranges found for the "quadruple pyrazolyl embrace". Our previous CSD database search revealed that this concerted set of noncovalent interactions occurred in approximately 25% of the cases where M(pz)$_2$X (M = metal, metalloid, X = C, B) is found.[2] The ranges of 3.0−4.6 Å (Cg···Cg), 4−28° (β slip angle) and 2.4−3.2 Å (CH···Cg), 120−160°

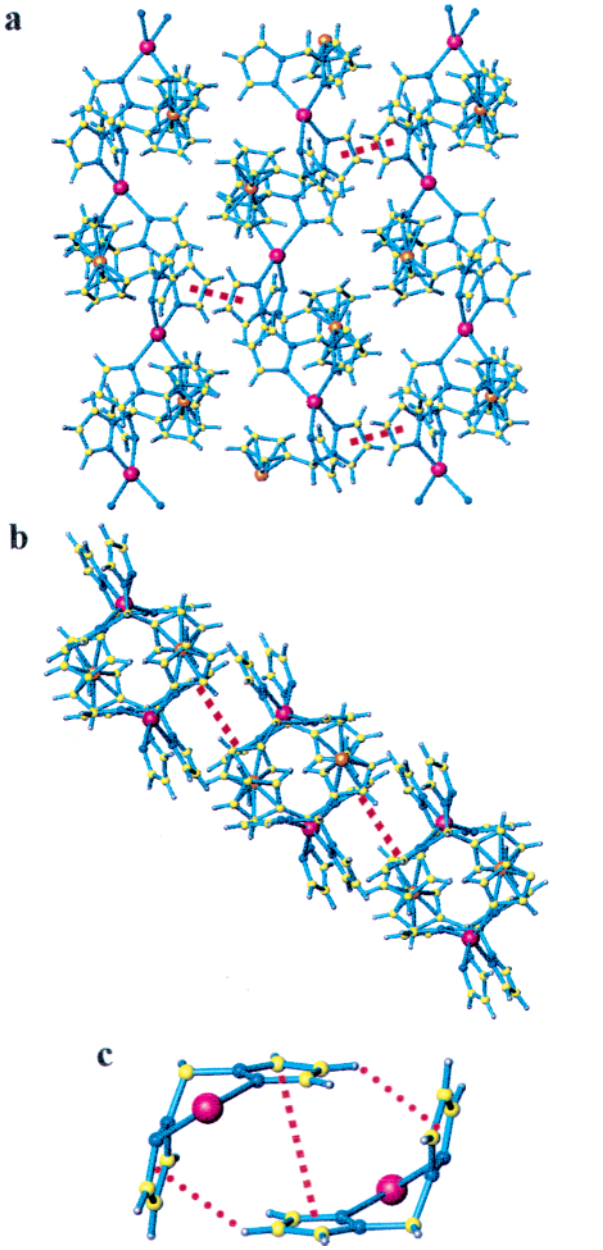

Figure 9. (a) Three helical chains of **3** held together by the $\pi\cdots\pi$ (red hashes) interaction of the pyrazolyl embrace (CH···π not shown). (b) View down the three chains arranged in a two-dimensional sheet by the pyrazolyl embrace. (c) Close-up view of the pyrazolyl embrace in **3** that holds the chains together into sheets. The CH···π interactions are shown as red dots.

(18) Grepioni, F.; Cojazzi, G.; Draper, S. M.; Scully, N.; Braga, D. *Organometallics* **1998**, *17*, 296.

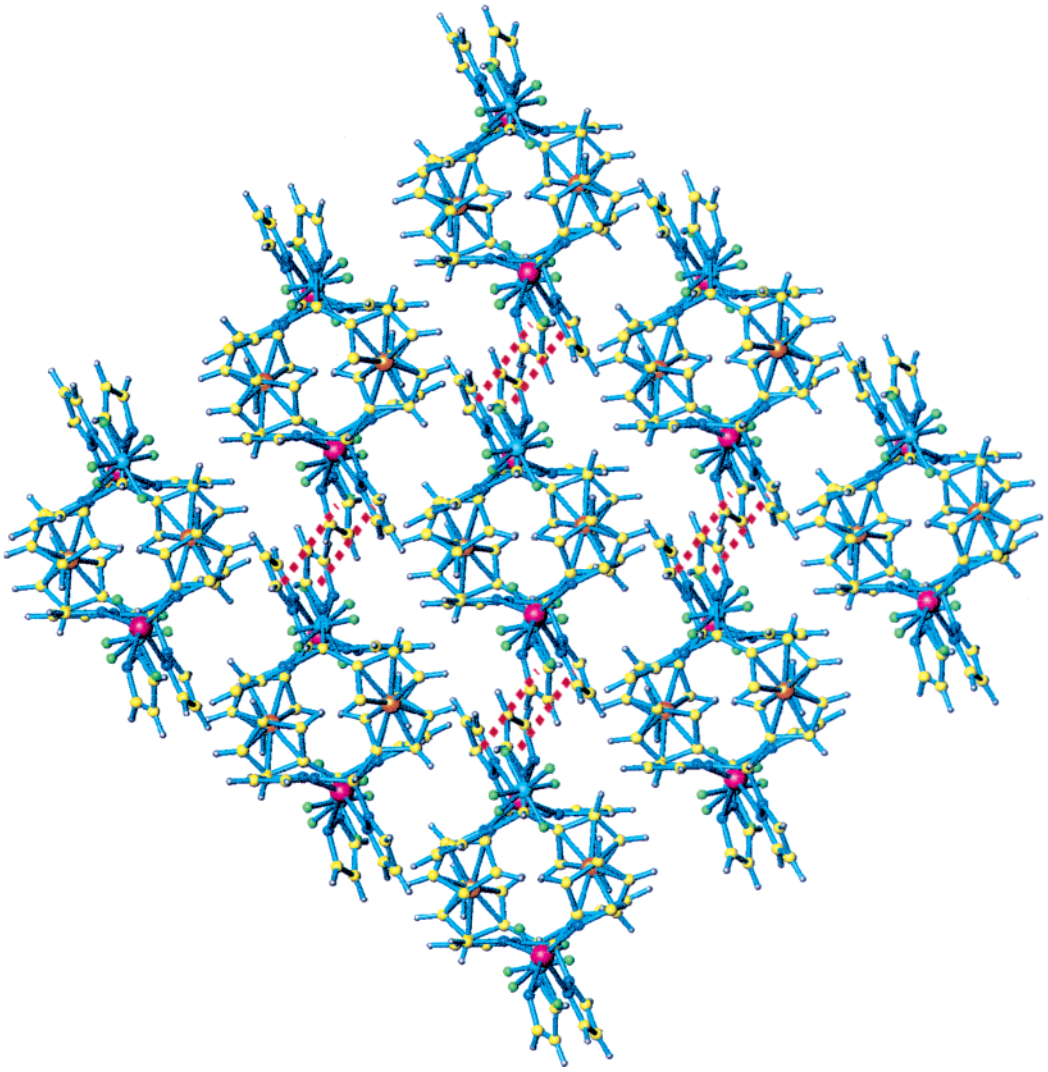

Figure 10. Three sheets of **3** held in a three-dimensional network by $\pi\cdots\pi$ (red hashes) interactions between chains of like chirality. The CH···F interactions which further hold the sheets in a three-dimensional array have been omitted for clarity.

(CH···Cg) were found for the $\pi\cdots\pi$ and CH···π components of the interaction, respectively, where the average values were 3.71 Å (Cg···Cg), 16.1° (β) and 2.76 Å (CH···Cg), and 141.6°(CH···Cg).

These sheets are further held into a three-dimensional array by $\pi\cdots\pi$ interactions. Figure 10 shows an end-on view of three sheets of **3** that form the three-dimensional array. While the Cg···Cg distance for the $\pi\cdots\pi$ interaction is slightly long at 4.09 Å, there are several $C_{pz}\cdots C_{pz}$ distances in the range of 3.29−3.77 Å. The three-dimensional structure is further supported by bifurcated CH···F interactions. The hydrogen atom at the 3-position of one of the pyrazolyl rings involved in the $\pi\cdots\pi$ interaction is directed toward two fluorine atoms of the nearby PF_6^- anion. The H(23)···F(4) distance is 2.44 Å with a C(23)···F(4) distance of 3.38 Å and a corresponding angle of 171°, while the H(23)···F(6) distance is 2.42 Å with a C(23)···F(6) distance of 3.07 Å and a corresponding angle of 126°.

$\{Fe[C_5H_4CH(pz)_2]_2AgPF_6\cdot{}^1/_2Et_2O\}_n$ ($3\cdot{}^1/_2Et_2O$). Unlike the chains in **3**, the one-dimensional chains in $3\cdot{}^1/_2Et_2O$ are nonhelical and run along the crystallographic *a* axis. Figure 11 shows two chains of $3\cdot{}^1/_2Et_2O$ that form two-dimensional sheets via several interactions with the PF_6^- anions, which lie in the gaps between neighboring chains rather than in the pockets of the chains as in **3**. One of the methine hydrogen atoms, H(1), and two hydrogen atoms, H(21) and H(41), at the 5-position of adjacent pyrazolyl groups of each chain are in close contact with fluorine atoms of the PF_6^- anion. The H(1)···F(1) distance is 2.43 Å with a C(1)···F(1) distance of 3.39 Å and a corresponding angle of 160°. The H(21)···F(6) and H(41)···F(2) distances are 2.37 and 2.46 Å with C(21)···F(6) and C(41)···F(2) distances of 3.27 and 3.37 Å and corresponding angles of 157 and 159°, respectively.

Figure 12 shows an end-on view of three sheets in $3\cdot{}^1/_2Et_2O$ that are held together in a three-dimensional network by CH···π interactions between two pyrazolyl rings from adjacent sheets. The H(12)···Cg distance illustrated by the red dotted line in Figure 12 is 2.70 Å with a C(12)···Cg distance of 3.60 Å and a corresponding angle of 158°. Disordered diethyl ether molecules reside between the sheets.

Summary

A new bitopic bis(pyrazolyl)methane ligand built around a ferrocene backbone has been prepared by the

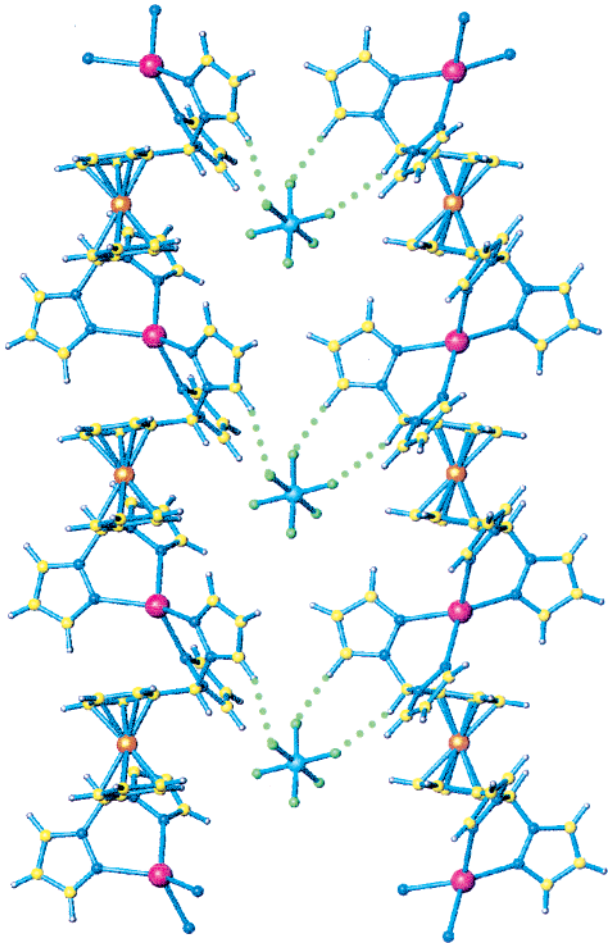

Figure 11. Two chains in $\mathbf{3}\cdot{}^1/_2Et_2O$ arranged by CH···F interactions (green dots) into a sheet.

$CoCl_2$-catalyzed rearrangement between 1,1′-ferrocenedicarbaldehyde and 1,1′-carbonyldipyrazole. This ligand has the conformational flexibility of a ferrocene group coupled with features designed to support supramolecular structures through weak hydrogen bonds, $\pi\cdots\pi$ stacking, and CH···π interactions. These organizing features are built into this family of poly(pyrazolyl)methane ligands by the presence of the aromatic pyrazolyl rings that can act as donors or acceptors in C−H···π interactions, can participate in $\pi\cdots\pi$ stacking, and can form weak hydrogen bonds as a result of interactions of the acidic hydrogen atoms of the pyrazolyl rings and the methine carbon with the anions used in this work.

The free ligand has a solid-state structure in which the bis(pyrazolyl)methane ligating sites are oriented 180° from one another in the solid state. The ligand is organized into a three-dimensional network in the crystal as a result of multiple noncovalent interactions of the acidic hydrogens of the pyrazolyl and methine groups with the nitrogen atoms and the π-cloud of the pyrazolyl rings. The silver(I) complexes of the new bitopic bis(pyrazolyl)methane ligand are bimetallic coordination polymers. In these complexes, the ferrocenyl groups no longer have the antiperiplanar eclipsed formation with $CH(pz)_2$ groups disposed 180°, but all six structures adopt a surprisingly similar conformation between synclinal eclipsed and anticlinal staggered where the angle between $CH(pz)_2$ groups is confined to the range of 85−99°. In all six structures, the silver pyrazolyl coordination spheres are also in a very similar distorted-tetrahedral arrangement.

The silver complexes were found to exist in two forms, helical and nonhelical forms. The main difference in the two structural types is the relative orientation of the ferrocenyl units in the polymer chains. In the helical form they are in an alternating AB orientation, whereas in the nonhelical form they are all in the same AA orientation. Both structural motifs have highly organized supramolecular structures organized by weak hydrogen bonds, $\pi\cdots\pi$ stacking, and CH···π interactions.

The complex $\{Fe[C_5H_4CH(pz)_2]_2AgPF_6\}_n$ (**3**) is unique in that crystals of each structural type, one containing solvent, have been grown. Figures 10 and 12 show the different crystal-packing arrangements for the two forms of **3** and are representative of all the compounds reported here. In the helical form, the chains are close-packed, with the anions residing in the pockets formed by the helices, and there are no solvent molecules present in the crystals. In the nonhelical form, the chains pack with sizable channels between them with the solvent molecules and the anions residing in the channels between the chains.

From the data reported here, it appears that the smaller anions (i.e. BF_4^- and PF_6^-) support the helical structure by fitting more easily into the spiral chains, but since both forms crystallize in the case of the PF_6^- anion, the size of the anion cannot be the only determining factor on whether the helical or nonhelical chain forms. Given the similarity of the arrangement of the ferrocene and silver coordination environments in the two types of structures, the relative energetics of the formation of the two structural types must be very similar. This result is surprising for two reasons. First, as outlined above, the packing arrangements are very different. Second, the chains in the helical structure are held together by the "quadruple pyrazolyl embrace" noncovalent interaction,[2] while this interaction is not present in the nonhelical cases. This interaction has been identified as a prevalent force organizing many structures containing poly(pyrazolyl)methane and poly(pyrazolyl)borate ligands[2] and would seem to favor the helical structural type. Clearly the open arrangement is also quite stable, as it is observed in four different structures formed from three different anions, PF_6^-, $SO_3CF_3^-$, and SbF_6^-, and two different solvents, diethyl ether and benzene.

Experimental Section

All operations were carried out under a nitrogen atmosphere using either standard Schlenk techniques or a Vacuum Atmospheres HE-493 drybox. All solvents were dried and distilled prior to use. 1,1′-Ferrocenedicarbaldehyde[10] and 1,1′-carbonyldipyrazole[11] were prepared according to literature procedures. Silver salts were purchased from Aldrich and used as received. Robertson Microlit Laboratories, Inc. (Madison, NJ), performed the elemental analyses. Reported temperatures for melting point determinations are uncorrected. ^1H (400 MHz) and ^{13}C (100.62 MHz) NMR chemical shifts are reported in ppm versus TMS and referenced to the residual solvent peaks for CD_3CN, δ 1.93 (^1H) and δ 1.39 (^{13}C). Mass spectrometric measurements were obtained on a MicroMass QTOF spectrometer using acetonitrile as the solvent.

Synthesis of 1,1′-Bis(dipyrazol-1-ylmethyl)ferrocene (1). A mixture of 0.78 g of 1,1′-carbonyldipyrazole (4.0 mmol),

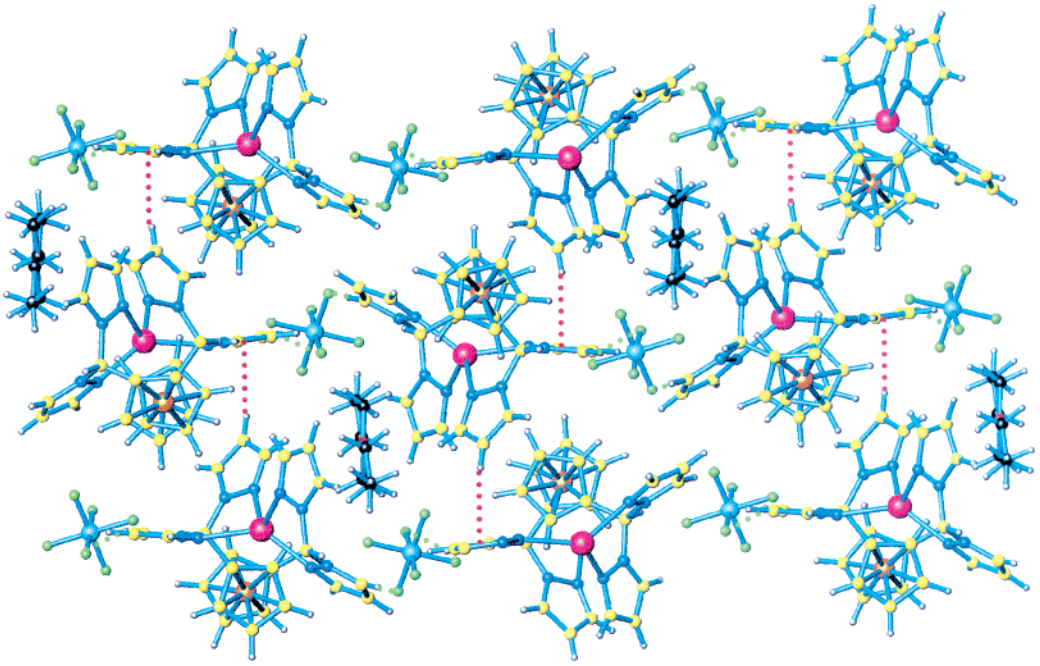

Figure 12. Two-dimensional sheets in **3**·$^1/_2Et_2O$ viewed down the chains organized by CH···F interactions (green dots). The three horizontal sheets are held together into a three-dimensional network by CH···π interactions (red dots). The trapped, disordered Et_2O molecules are shown as black spheres.

0.53 g (1.8 mmol) of 1,1′-ferrocenedicarbaldehyde, and 86 mg of $CoCl_2$ in 20 mL of toluene was heated under N_2 at reflux for 5 h. After the reaction mixture had cooled to room temperature, water (20 mL) was added and the mixture was stirred for 30 min. The organic layer was separated, and the aqueous layer was extracted with CH_2Cl_2 (3 × 50 mL). The combined organic fractions were washed with a saturated brine solution (50 mL) and separated. The brine solution was further extracted with CH_2Cl_2 (4 × 100 mL). All of the organic fractions were combined and dried over $MgSO_4$. After filtration to remove the drying agent, most of the solvent was removed via rotary evaporation, leaving primarily toluene. Silica gel (20 g) was added, and the mixture was evaporated to dryness. The residue was loaded onto a silica gel column and eluted with diethyl ether. When the yellow band started to elute, the column was then flushed with THF. A 0.75 g (72% yield) sample of pure **1** was obtained as an orange crystalline solid after removing the solvent from the yellow band, mp 184−186 °C dec. ^{1}H NMR (CD_3CN): 7.67, 7.50 (dd, dd, J = 2.6, 1.8 Hz, 2H, 2H, $H_{3,5}$ pz), 7.36 (s, 1H, C_α H), 6.26 (dd, J = 2.2 Hz, 2H, H_4 pz), 4.36 (m, 2H, Cp H), 4.09 (m, 2H, Cp H). ^{13}C NMR (CD_3CN): 140.7 (C_5 pz), 130.2 (C_3 pz), 106.8 (C_4 pz), 86.1 (C_α), 75.4, 71.1, 70.8 (Cp's). ESI$^+$ HRMS (*m*/*z*): $[M]^+$ calcd for $[C_{24}H_{22}FeN_8]^+$, 478.1317; found, 478.1321. ESI$^+$ MS (*m*/*z* (relative intensity, %) [assignment]): 478 (12) $[M]^+$, 411 (100) $[M - pz]^+$, 343 (6) $[M - pz - Hpz]^+$, 275 (5) $[M - pz - 2Hpz]^+$. Anal. Calcd for $C_{24}H_{22}N_8Fe$: C, 60.26; H, 4.64; N, 23.43. Found: C, 59.99; H, 4.45; N, 23.20. Crystals suitable for X-ray diffraction studies were grown by layering a saturated acetone solution of **1** with hexane.

Synthesis of $[Ag\{Fe[C_5H_4CH(pz)_2]\}]_n(BF_4)_n$ (2). A solution of 0.040 g (0.21 mmol) of $AgBF_4$ in THF (10 mL) was added by cannula to a solution of 0.10 g (0.21 mmol) of **1** in THF (15 mL). After the reaction mixture had been stirred at room temperature in the dark for 2 h, the resulting yellow precipitate was isolated by cannula filtration. The yellow insoluble solid was washed with two 5 mL portions of diethyl ether and was dried under vacuum to afford the desired compound as a yellow powder in 75% yield (0.11 g), mp 192−195 °C dec. ^{1}H NMR (CD_3CN): 7.80, 7.53 (d, d, J = 2.0, 1.2 Hz, 2H, 2H, $H_{3,5}$ pz), 7.50 (s, 1H, C_α H), 6.32 (dd, J = 2.4, 2.0 Hz, 2H, H_4 pz), 4.33 (m, 2H, Cp H), 4.13 (m, 2H, Cp H). ^{13}C NMR (CD_3CN): 141.8 (C_5 pz), 131.2 (C_3 pz), 107.1 (C_4 pz), 85.8 (C_α), 75.0, 71.3, 70.7 (Cp's). ESI$^+$ MS (*m*/*z* (relative intensity, %) [assignment]): 1259 (33) $[Ag_2L_2BF_4]^+$, 1063 (5) $[AgL_2]^+$, 585 (100) $[AgL]^+$, 411 (58) $[L - pz]^+$, 343 (29) $[L - pz - Hpz]^+$. Anal. Calcd for $C_{24}H_{22}N_8FeAgBF_4$: C, 42.83; H, 3.29; N, 16.65. Found: C, 42.50; H, 2.97; N, 16.39. Crystals suitable for X-ray structural studies and analytical figures were obtained by vapor diffusion of diethyl ether into an acetonitrile solution of **2**.

Synthesis of $[Ag\{Fe[C_5H_4CH(pz)_2]\}]_n(PF_6)_n$ (3). Compound **3** was prepared (0.31 g, 83%) as described above for **2** using $AgPF_6$ (0.13 g, 0.52 mmol) and **1** (0.25 g, 0.52 mmol), mp 198−200 °C dec. ^{1}H NMR (CD_3CN): 7.71, 7.51 (d, d, J = 2.0, 0.8 Hz, 2H, 2H, $H_{3,5}$ pz), 7.41 (s, 1H, C_α H), 6.28 (dd, J = 2.0, 2.0 Hz, 2H, H_4 pz), 4.35 (m, 2H, Cp H), 4.11 (m, 2H, Cp H). ^{13}C NMR (CD_3CN): 142.2 (C_5 pz), 131.6 (C_3 pz), 107.2 (C_4 pz), 85.7 (C_α), 74.9, 71.4, 70.6 (Cp's). ESI$^+$ MS (*m*/*z* (relative intensity, %) [assignment]): 1317 (19) $[Ag_2L_2PF_6]^+$, 1063 (4) $[AgL_2]^+$, 585 (100) $[AgL]^+$, 411 (38) $[L - pz]^+$, 343 (22) $[L - pz - Hpz]^+$. Anal. Calcd for $C_{24}H_{22}N_8FeAgPF_6$: C, 39.42; H, 3.03; N, 15.33. Found: C, 39.07; H, 2.79; N, 15.12. Crystals suitable for X-ray structural studies were obtained by vapor diffusion of diethyl ether into an acetonitrile solution of **3**.

Synthesis of $[Ag\{Fe[C_5H_4CH(pz)_2]\}]_n(CF_3SO_3)_n$ (4). Compound **4** was prepared (0.16 g, 95%) as described above for **2** using $Ag(CF_3SO_3)$ (0.58 g, 0.23 mmol) and **1** (0.11 g, 0.23 mmol), mp 180−182 °C dec. ^{1}H NMR (CD_3CN): 7.79, 7.53 (d, d, J = 2.4, 1.6 Hz, 2H, 2H, $H_{3,5}$ pz), 7.49 (s, 1H, C_α H), 6.31-(dd, J = 2.4, 1.6 Hz, 2H, H_4 pz), 4.33 (m, 2H, Cp H), 4.13 (m, 2H, Cp H). ^{13}C NMR (CD_3CN): 141.7 (C_5 pz), 131.1 (C_3 pz), 107.0 (C_4 pz), 85.8 (C_α), 75.0, 71.2, 70.7 (Cp's). ESI$^+$ MS (*m*/*z* (relative intensity, %) [assignment]): 1321 (81) $[Ag_2L_2OTf]^+$, 1063 (5) $[AgL_2]^+$, 843 (51) $[Ag_2LOTf]^+$, 585 (100) $[AgL]^+$, 411 (26) $[L - pz]^+$, 343 (13) $[L - pz - Hpz]^+$. Anal. Calcd for $C_{25}H_{22}N_8AgF_3FeO_3S$: C, 40.84; H, 3.02; N, 15.24. Found: C, 40.62; H, 2.78; N, 14.98. Crystals suitable for X-ray structural studies were obtained by layering benzene with an acetonitrile solution of **4**.

Synthesis of $[Ag\{Fe[C_5H_4CH(pz)_2]\}]_n(SbF_6)_n$ (5). Compound **5** was prepared (0.38 g, 88%) as described above for **2** using $AgSbF_6$ (0.18 g, 0.52 mmol) and **1** (0.25 g, 0.52 mmol),

Table 2. Selected Bond Lengths (Å) and Angles (deg) for 2, 3, 3·½Et₂O, 4·1.5C₆H₆, 5·½Et₂O, and 5·½C₆H₆

	2	3	3·½Et₂O	4·1.5C₆H₆	5·½Et₂O	5·½C₆H₆
Ag−N(11)	2.284(3)	2.260(2)	2.407(3)	2.382(4)	2.420(4)	2.285(3)
Ag−N(21)	2.352(3)	2.384(2)	2.257(3)	2.230(3)	2.260(3)	2.375(3)
Ag−N(31)	2.278(3)	2.280(3)	2.364(3)	2.400(4)	2.384(4)	2.265(3)
Ag−N(41)	2.361(3)	2.367(2)	2.246(3)	2.225(3)	2.248(4)	2.379(3)
N(11)−Ag−N(21)	84.78(10)	84.73(8)	82.53(10)	85.64(12)	82.26(12)	82.02(9)
N(11)−Ag−N(31)	136.19(10)	136.39(9)	110.64(10)	100.95(13)	109.06(13)	129.61(10)
N(11)−Ag−N(41)	117.11(10)	121.75(9)	128.87(11)	120.10(13)	127.90(13)	119.01(9)
N(21)−Ag−N(31)	129.96(11)	126.76(9)	115.99(11)	118.48(12)	117.55(13)	128.31(10)
N(21)−Ag−N(41)	108.79(10)	107.23(8)	135.46(11)	143.74(13)	136.92(14)	119.31(9)
N(31)−Ag−N(41)	80.12(10)	80.83(9)	84.67(11)	83.57(12)	84.10(13)	83.35(9)

Table 3. Crystal Data and Structure Refinement Information for Compounds 1−5

	1	2	3	3·½Et₂O	4·1.5C₆H₆	5·½Et₂O	5·½C₆H₆
empirical formula	$C_{24}H_{22}FeN_8$	$C_{24}H_{22}AgBF_4FeN_8$	$C_{24}H_{22}AgF_6FeN_8P$	$C_{26}H_{27}AgF_6FeN_8O_{0.50}P$	$C_{34}H_{31}AgF_3FeN_8O_3S$	$C_{26}H_{27}AgF_6FeN_8O_{0.5}Sb$	$C_{27}H_{25}AgF_6FeN_8Sb$
formula wt	478.35	673.03	731.19	768.25	852.45	859.03	861.02
temp, K	150(2)	150(2)	150(2)	150(2)	150(2)	293(2)	293(2)
cryst syst	triclinic	monoclinic	monoclinic	monoclinic	monoclinic	monoclinic	monoclinic
space group	*P*1	$P2_1/n$	$P2_1/n$	$P2_1/n$	$P2_1/c$	$P2_1/n$	$P2_1/n$
unit cell dimens							
a, Å	7.6843(5)	11.9318(5)	12.3933(6)	9.4970(5)	10.0253(5)	9.6115(7)	9.7092(5)
b, Å	11.1955(8)	14.8171(7)	15.2016(7)	22.3716(11)	16.6008(8)	22.9599(18)	14.1361(7)
c, Å	13.2050(9)	14.5865(7)	14.2888(7)	13.7001(7)	20.7934(11)	13.9949(11)	22.2926(12)
α, deg	82.6320(10)	90	90	90	90	90	90
β, deg	87.2810(10)	91.3570(10)	90.5770(10)	100.0720(10)	96.1270(10)	101.040(2)	97.7720(10)
γ, deg	70.2050(10)	90	90	90	90	90	90
V, Å³	1060.06(13)	2578.1(2)	2691.8(2)	2865.9(3)	3440.8(3)	3031.2(4)	3031.6(3)
Z	2	4	4	4	4	4	4
density (calcd), Mg m^{-3}	1.499	1.734	1.804	1.781	1.646	1.882	1.886
abs coeff, mm^{-1}	0.743	1.382	1.399	1.320	1.116	2.068	2.067
cryst size, mm³	0.46 × 0.26 × 0.20	0.24 × 0.10 × 0.04	0.62 × 0.20 × 0.14	0.26 × 0.14 × 0.08	0.28 × 0.22 × 0.06	0.36 × 0.20 × 0.03	0.28 × 0.20 × 0.08
θ range for data collecn, deg	1.55−26.42	1.96−25.05	1.96−26.40	1.76−26.41	1.57−24.41	1.73−25.02	1.71−26.38
index ranges	$-9 \le h \le 9$ $-14 \le k \le 14$ $-16 \le l \le 16$	$-14 \le h \le 14$ $-17 \le k \le 17$ $-17 \le l \le 17$	$-15 \le h \le 15$ $-18 \le k \le 18$ $-17 \le l \le 17$	$-11 \le h \le 11$ $-27 \le k \le 28$ $-17 \le l \le 17$	$-11 \le h \le 11$ $-19 \le k \le 19$ $-24 \le l \le 24$	$-11 \le h \le 11$ $-27 \le k \le 27$ $-16 \le l \le 16$	$-12 \le h \le 12$ $-17 \le k \le 17$ $-27 \le l \le 27$
no. of rflns collected	8698	18 718	19 179	25 695	26 092	24 956	27 681
no. of indep rflns (*R*(int))	4322 (0.0201)	4565 (0.0428)	5504 (0.0314)	5868 (0.0324)	5665 (0.0411)	5351 (0.0393)	6207 (0.0316)
completeness to θ_{max}, %	99.30	99.80	99.70	99.80	100.00	100.00	99.90
abs cor	semiempirical from equiv						
max/min transmissn	1.0000/0.8343	1.0000/0.7615	1.0000/0.8358	1.0000/0.8101	1.0000/0.7564	1.0000/0.7589	1.0000/0.7592
no. of data/restraints/params	4322/0/329	4565/10/383	5504/0/370	5868/14/403	5665/61/552	5351/14/403	6207/0/397
goodness of fit on F^2	1.042	1.092	1.038	1.062	1.053	1.022	1.025
final *R* indices ($I > 2\sigma(I)$)							
R1	0.0332	0.0400	0.0369	0.0438	0.0472	0.0395	0.0320
wR2	0.0860	0.0849	0.0861	0.1071	0.1021	0.0923	0.0772
R indices (all data)							
R1	0.0360	0.0510	0.0458	0.0481	0.0550	0.0495	0.0387
wR2	0.0880	0.0894	0.0902	0.1101	0.1066	0.0981	0.0810
largest diff peak/hole, e Å^{-3}	0.381/−0.402	0.782/−0.310	1.128/−0.421	1.125/−0.982	0.751/−0.406	0.839/−0.545	1.080/−0.477

mp 221−223 °C dec. ^{1}H NMR (CD_3CN): 7.80, 7.53 (d, d, J = 2.4, 1.6 Hz, 2H, 2H, $H_{3,5}$ pz), 7.50 (s, 1H, C_α H), 6.32 (dd, J = 2.0, 2.4 Hz, 2H, H_4 pz), 4.32 (m, 2H, Cp H), 4.14 (m, 2H, Cp H). ^{13}C NMR (CD_3CN): 141.9 (C_5 pz), 131.3 (C_3 pz), 107.1 (C_4 pz), 85.7 (C_α), 75.0, 71.3, 70.7 (Cp's). ESI$^+$ MS (*m*/*z* (relative intensity, %) [assignment]):1407 (21) $[Ag_2L_2SbF_6]^+$, 1063 (44) $[AgL_2]^+$, 585 (100) $[AgL]^+$, 411 (55) $[L - pz]^+$. Anal. Calcd for $C_{24}H_{22}N_8FeAgSbF_6$: C, 35.07; H, 2.70; N, 13.63. Found: C, 34.95; H, 2.52; N, 13.39. Crystals suitable for X-ray structural studies were obtained by vapor diffusion of diethyl ether into an acetonitrile solution of **5**, giving **5**·½Et_2O, and by layering benzene with an acetonitrile solution of **5**, giving **5**·½C_6H_6.

Crystallographic Studies. Single crystals for X-ray diffraction studies were grown for each compound as described above. In the case of **3**, two types of crystals formed from the same stock acetonitrile solution. The crystals, **3** and **3**·½Et_2O, were grown in the same larger vial but formed in different inner vials. Crystal data and data collection and refinement parameters are given in Table 3.

A bright yellow block of **1**, a yellow bar of **2**, a long yellow bar of **3**, a yellow block of **3**·½Et_2O, and a yellow plate of **4**·1.5C_6H_6 were mounted on the ends of thin glass fibers using inert oil and quickly transferred to the diffractometer cold stream for data collection at 150(2) K. A yellow plate of **5**·½Et_2O and a yellow block of **5**·½C_6H_6 were also mounted for X-ray data collection at 293(2) K. Raw X-ray intensity data frames were measured on a Bruker SMART APEX CCD-based diffractometer system (Mo Kα radiation, λ = 0.710 73 Å). The raw data frames were integrated using SAINT+,[19] which also applied corrections for Lorentz and polarization effects. Analysis of the data sets showed negligible crystal decay during data collection in any case. An empirical absorption correction based on the multiple measurement of equivalent reflections was applied to each data set with the program SADABS.[19] All structures were solved by a combination of direct methods and difference Fourier syntheses and refined by full-matrix least squares against F^2, using the SHELXTL software package.[20] Non-hydrogen atoms were refined with anisotropic displace-

ment parameters, and hydrogen atoms were placed in geometrically idealized positions and included as riding atoms with refined isotropic displacement parameters, unless otherwise noted.

$Fe(C_5H_4CH(pz)_2)_2$ (**1**) crystallizes in the triclinic space group $P\bar{1}$. The asymmetric unit consists of half each of two independent molecules, both located on inversion centers. Hydrogen atoms H(1) and H(31) were located and refined freely.

$\{Fe(C_5H_4CH(pz)_2)_2AgBF_4\}_n$ (**2**) crystallizes in the monoclinic space group $P2_1/n$ based on systematic absences. The asymmetric unit contains one Ag atom, one $Fe(C_5H_4CH(pz)_2)_2$ ligand, and a BF_4^- anion which is disordered over two sites in the ratio 0.58(1)/0.42. A total of 10 geometric restraints (SHELX SAME) were used to model the anion disorder.

$\{Fe(C_5H_4CH(pz)_2)_2AgPF_6\}_n$ (**3**) crystallizes in the monoclinic space group $P2_1/n$ based on systematic absences. The asymmetric unit contains one Ag atom, one $Fe(C_5H_4CH(pz)_2)_2$ ligand, and one PF_6^- anion.

$\{Fe(C_5H_4CH(pz)_2)_2AgPF_6 \cdot {}^1/_2Et_2O\}_n$ (**3**$\cdot{}^1/_2Et_2O$) crystallizes in the monoclinic space group $P2_1/n$ based on systematic absences. The asymmetric unit contains the Ag atom, one $Fe(C_5H_4CH(pz)_2)_2$ ligand, one PF_6^- anion, and half of an Et_2O molecule of crystallization which is disordered about an inversion center. A total of 14 restraints were used to maintain a chemically reasonable geometry for this species.

$\{Fe(C_5H_4CH(pz)_2)_2AgCF_3SO_3 \cdot 1.5C_6H_6\}_n$ (**4**$\cdot 1.5C_6H_6$) crystallizes in the monoclinic space group $P2_1/c$ based on systematic absences. The asymmetric unit contains one Ag atom, one $Fe(C_5H_4CH(pz)_2)_2$ ligand, a $SO_3CF_3^-$ anion which is disordered over two nearby sites in the ratio 0.74(1)/0.26, half of a benzene molecule of crystallization located on a inversion center, and another benzene which is equally disordered over two positions. Both components of the disordered benzene were fitted to a regular hexagon of variable size. A total of 61 geometric restraints (SHELX SADI) were used to model the anion disorder.

$\{Fe(C_5H_4CH(pz)_2)_2AgSbF_6 \cdot {}^1/_2Et_2O\}_n$ (**5**$\cdot{}^1/_2Et_2O$) crystallizes in the monoclinic space group $P2_1/n$ based on systematic absences. The asymmetric unit contains one Ag atom, one $Fe(C_5H_4CH(pz)_2)_2$ ligand, one SbF_6^- anion, and half of an Et_2O molecule of crystallization which is disordered about an inversion center. A total of 14 restraints were used to maintain a chemically reasonable geometry for this species.

$\{Fe(C_5H_4CH(pz)_2)_2AgSbF_6 \cdot {}^1/_2Et_2O\}_n$ (**5**$\cdot{}^1/_2C_6H_6$) crystallizes in the monoclinic space group $P2_1/c$ based on systematic absences. The asymmetric unit contains one Ag atom, one $Fe(C_5H_4CH(pz)_2)_2$ ligand, one SbF_6^- anion, and half of a benzene molecule of crystallization located on an inversion center.

Crystallographic data for the structural analyses has been deposited with the Cambridge Crystallographic Centre: CCDC 209079 for compound **1**, CCDC 209080 for compound **2**, CCDC 209081 for compound **3**, CCDC 209082 for compound **3**$\cdot{}^1/_2Et_2O$, CCDC 209083 for compound **4**$\cdot 1.5C_6H_6$, CCDC 212006 for compound **5**$\cdot{}^1/_2Et_2O$, and CCDC 212007 for compound **5**$\cdot{}^1/_2C_6H_6$. Copies of this information may be obtained free of charge from the director, CCDC, 12 Union Road, Cambridge, CB2 1EZ U.K. (fax, +44-1223-336-033; e-mail, deposit@ccdc.cam.ac.uk; web, www: http://www.ccdc.cam.ac.uk).

Acknowledgment. We thank the National Science Foundation (Grant No. CHE-0110493) for support. The Bruker CCD single crystal diffractometer was purchased using funds provided by the NSF Instrumentation for Materials Research Program through Grant DMR:9975623. The NSF (Grant Nos. CHE-8904942 and CHE-9601723) and NIH (Grant No. RR-02425) have supplied funds to support NMR equipment, and the NIH (Grant No. RR-02849) has supplied funds to support mass spectrometry equipment at the University of South Carolina.

Supporting Information Available: Text giving a discussion and figures giving the supramolecular structures of **2**, **4**$\cdot 1.5C_6H_6$, **5**$\cdot{}^1/_2Et_2O$, and **5**$\cdot{}^1/_2C_6H_6$ and tables of structure refinement parameters, atomic coordinates, bond distances, bond angles, and anisotropic thermal parameters for these compounds. This material is available free of charge via the Internet at http://pubs.acs.org.

OM0305216

(19) SMART Version 5.625, SAINT+ Version 6.02a, and SADABS; Bruker Analytical X-ray Systems, Inc., Madison, WI, 1998.

(20) Sheldrick, G. M. SHELXTL Version 5.1; Bruker Analytical X-ray Systems, Inc., Madison, WI, 1997.